

ON THE DISKS OF SPIRAL AND S0 GALAXIES

K. C. FREEMAN

Mount Stromlo and Siding Spring Observatories, Research School of Physical Sciences,
 Australian National University

Received 1969 August 19; revised 1969 December 8

ABSTRACT

Surface photometry shows that most spiral and S0 galaxies have two main components: a spheroidal component, and an exponential disk component with radial surface-brightness distribution $I(R) = I_0 e^{-aR}$. The exponential disk is the subject of this paper. First, for the exponential disk in centrifugal equilibrium with surface density $\mu(R) = \mu_0 e^{-aR}$, we derive the circular-velocity field and the mass-angular momentum distribution $\mathcal{M}(h)$; $\mathcal{M}(h)$ is the total mass with angular momentum per unit mass less than h . $\mathcal{M}(h)$ for the exponential disk is almost identical with $\mathcal{M}(h)$ for a family of rigidly rotating spheres of uniform density. We then collect photometric data for the disks of thirty-six spiral and S0 galaxies, and find the following: (i) Twenty-eight of the thirty-six galaxies have approximately the same intensity scale I_0 (21.65 B -mag per square second of arc), with a standard deviation of only 0.30 mag per square second of arc, despite a range of nearly 5 mag in absolute magnitude. This constancy of I_0 produces the correlation between apparent magnitude and angular diameter found by Hubble. (ii) S0-Sbc systems have any value of the disk length scale a^{-1} between 1 and 5 kpc, while later-type systems have predominantly low values of a^{-1} (< 2 kpc). (iii) The relative brightness and size of the spheroidal and disk components are only weakly correlated with morphological type.

If conclusion (i) implies that μ_0 is approximately constant, then the disk's total mass \mathcal{M} and angular momentum \mathcal{S} satisfy $\mathcal{S} \propto \mathcal{M}^{7/4}$. If $\mathcal{M}(h)$ is invariant as a protogalaxy collapses to form a galaxy, then all protogalaxies destined to be S0 or spiral galaxies have a similar $\mathcal{M}(h)$ (in dimensionless variables), at least for the range of h corresponding to the disk. If $\mathcal{M}(h)$ is not invariant, then there exists a very efficient mechanism which establishes the characteristic $\mathcal{M}(h)$ for these systems as they form.

The exponential nature of the disk is not defined by $\mathcal{M}(h)$ alone; its cause remains uncertain.

I. INTRODUCTION

Figure 1 shows the radial distribution of the surface brightness $I(R)$ in M83 (SAB(s)c [Sersic 1969]) and NGC 4459 (SA(r)0 [Liller 1960]). These are typical light distributions for the whole family of disklike galaxies, which includes the Magellanic-type irregulars and the spiral and lenticular (S0) systems (Sandage, Freeman, and Stokes 1970). De Vaucouleurs (1959a) has pointed out that the $I(R)$ distributions for these galaxies show two main components: an inner *spheroidal* component which follows fairly closely his law

$$\log I \propto R^{1/4} \quad (1)$$

and an outer *exponential* component (disk), with

$$I(R) = I_0 e^{-aR}, \quad (2)$$

which contributes a large part of the total light and angular momentum. For example, in M31, which has a fairly prominent spheroidal component, more than 75 percent of the blue light (de Vaucouleurs 1958) and probably more than 95 percent of the total angular momentum (Takase 1967) come from this exponential disk. The spheroidal component may be prominent as in M31, or very weak as in M33 (de Vaucouleurs 1959b).

The two-component nature of $I(R)$ for disk systems distinguishes them from the normal elliptical galaxies. The ellipticals have a single-component luminosity distribution which follows closely the $R^{1/4}$ law of equation (1) (de Vaucouleurs 1959a). Note that this $R^{1/4}$ distribution itself appears approximately exponential for large R , so the $I(R)$ law in the outer parts of ellipticals is *qualitatively* similar to that shown in Figure 1 for

the S0 system NGC 4459. However, the important difference between the $I(R)$ distributions for elliptical and disk galaxies is that, because the ellipticals are really one-component systems conforming to the $R^{1/4}$ law, the apparently exponential and nonexponential parts of their $I(R)$ profiles are *not* independent. For example, the fraction of the total light emitted within the nonexponential part of the $I(R)$ distribution is approximately the same for all ellipticals; this is certainly not true for disk galaxies (see § III).

Almost every disklike galaxy with measured $I(R)$ shows an *exponential* disk (see de Vaucouleurs 1959*a* and the references for Table 1). This disk is probably the most general property of these galaxies, and its origin is certainly a significant cosmogonic problem. It seems surprising that this problem has been almost ignored so far, whereas there is an extensive literature on the $I(R)$ distribution for elliptical galaxies. The problem of the exponential disk is the subject of this paper.

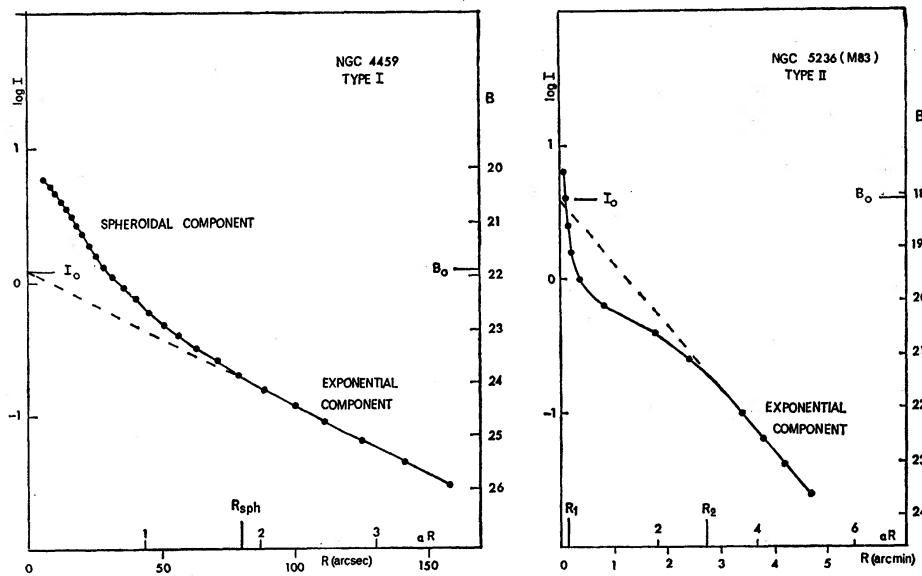


FIG. 1.—Radial luminosity distributions for NGC 4459 and M83. I is the surface brightness. Ordinates are $\log I$ and I in B -mag per square second of arc. R is distance from the nucleus along the major axis; the dimensionless radius aR is also shown. I_0 , B_0 are the surface-brightness scale for the exponential disk, uncorrected for inclination and galactic absorption. R_1 , R_2 , and R_{sph} are defined in § III. Filled circles, observed points.

Before we can understand the exponential disks, it is necessary to gather dynamical and observational information about them. In § II we show that it is reasonable to assume that $I(R) = I_0 e^{-aR}$ implies a surface-density distribution

$$\mu(R) = \mu_0 e^{-aR} \quad (3)$$

in the disk. Then dynamical functions such as the circular-velocity field and the mass-angular momentum distribution are derived for the exponential disk of equation (3) in centrifugal equilibrium. The main results of this paper are in § III, where we collect data for thirty-six disklike systems with well-defined exponential components. The implications of these results are discussed in § IV.

II. DYNAMICAL PROPERTIES OF THE DISK

First we need to know whether $I(R) = I_0 e^{-aR}$ implies a surface-density distribution $\mu(R) = \mu_0 e^{-aR}$. Only a few galaxies have two-color surface photometry extending into

the disk; from the approximate radial uniformity of $B - V$ in the disks of M33, M31, NGC 1332, and the LMC (see references for Table 1), we infer that the mass/luminosity ratio is approximately uniform, at least within the disk of any one galaxy (cf. Schwarzschild 1954), and that the exponential surface-density distribution of equation (3) holds for the disks.

Now we compute some dynamical quantities for the exponential disk of equation (3) in centrifugal equilibrium. They include (a) the circular-velocity field, (b) the total angular momentum, (c) the Lindblad-resonance frequencies, and (d) the mass-angular momentum distribution. Some of these quantities will be useful for the discussion of the observational data presented in § III.

a) The Rotation Curve

We first compute the rotation curve for the zero-thickness exponential disk in centrifugal equilibrium. Toomre's (1963) method is ideal for this disk. He writes the surface density $\mu(R)$ as the Bessel integral

$$\mu(R) = \int_0^{\infty} J_0(kR) k S(k) dk, \quad (4)$$

where

$$S(k) = \int_0^{\infty} J_0(kR) u \mu(u) du. \quad (5)$$

It then follows from Poisson's equation that the radial gradient of the gravitational potential Φ in the plane of the disk is

$$-\left(\frac{\partial \Phi}{\partial R}\right)_{z=0} = 2\pi G \int_0^{\infty} J_1(Rk) k S(k) dk. \quad (6)$$

From the centrifugal-equilibrium condition

$$\frac{V^2(R)}{R} = -\left(\frac{\partial \Phi}{\partial R}\right)_{z=0}, \quad (7)$$

where $V(R)$ is the circular velocity at radius R , it follows that

$$\frac{V^2(R)}{R} = 2\pi G \int_0^{\infty} J_1(Rk) k \int_0^{\infty} J_0(ku) u \mu(u) du dk \quad (8)$$

$$= 2\pi G \mu_0 \int_0^{\infty} J_1(Rk) k \int_0^{\infty} u e^{-au} J_0(ku) du dk \quad (9)$$

for the exponential disk, where G is the gravitational constant.

From equation (6) of Watson (1944, p. 386) and formula (6.552) of Gradshteyn and Ryzhik (1965), it is possible to show that

$$\frac{V^2(R)}{R} = \pi G \mu_0 a R (I_0 K_0 - I_1 K_1), \quad (10)$$

where I and K are modified Bessel functions (see Watson 1944, p. 77) and are evaluated at $\frac{1}{2} a R$.

The total mass of the exponential disk is

$$\mathfrak{M} = 2\pi \mu_0 / a^2. \quad (11)$$

The rotation curve of equation (10) can be written in dimensionless form: let $\tilde{R} = aR$ and $\tilde{V} = V/\sqrt{GMa}$. Then equation (10) becomes

$$\tilde{V}^2(\tilde{R}) = \frac{1}{2}\tilde{R}^2[I_0(\frac{1}{2}\tilde{R})K_0(\frac{1}{2}\tilde{R}) - I_1(\frac{1}{2}\tilde{R})K_1(\frac{1}{2}\tilde{R})]. \quad (12)$$

This rotation curve is shown in Figure 2. The dimensionless Keplerian curve is included for comparison; note how slowly the curve of equation (12) approaches the asymptotic Keplerian velocity law (cf. Toomre 1963).

We can compare the rotation curve shown in Figure 2 with those observed in the few systems with available rotation curves and surface photometry, and with weak spheroidal components, so that the gravitational field is dominated by the disk over most of the galaxy. This comparison is made in Appendix A.

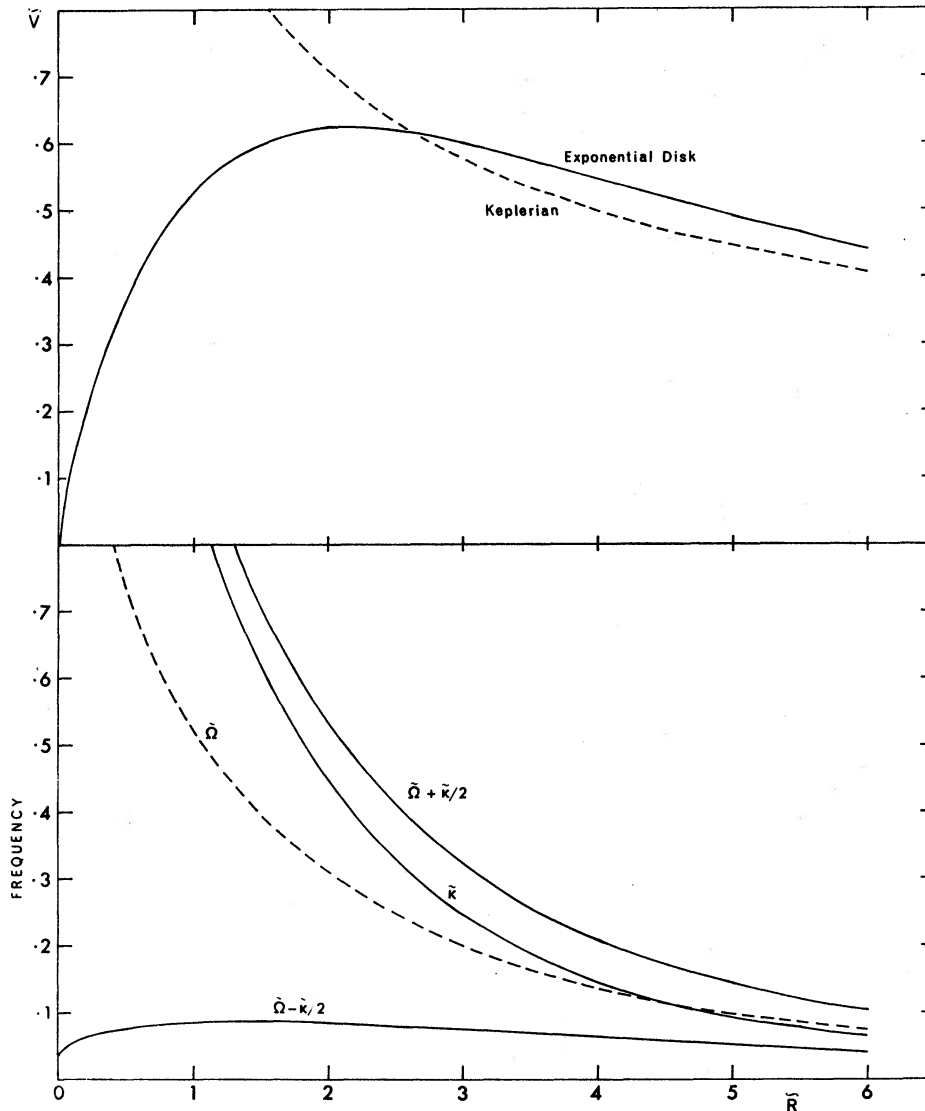


FIG. 2 (top).—Dimensionless rotation curve for the exponential disk. \tilde{V} and \tilde{R} are defined in § IIa. Broken line shows the corresponding Keplerian curve.

FIG. 3 (bottom).—Dimensionless angular velocity, epicyclic frequency, and Lindblad-resonance frequencies for the exponential disk (see § IIc).

b) *The Total Angular Momentum*

The total angular momentum for the exponential disk is

$$\begin{aligned} \mathfrak{S} &= \int_0^{\infty} 2\pi R \mu(R) V(R) R dR \\ &= (GM^3/a)^{1/2} \int_0^{\infty} \tilde{V} \tilde{R}^2 \exp(-\tilde{R}) d\tilde{R} \end{aligned} \quad (13)$$

where $\tilde{V}(\tilde{R})$ is given in equation (12). Numerical integration then gives

$$\mathfrak{S} = 1.109(GM^3/a)^{1/2}. \quad (14)$$

There is only one exponential disk with a given total mass \mathfrak{M} and total angular momentum \mathfrak{S} .

c) *Lindblad-Resonance Frequencies*

Lin and Shu (1966) show that a density-wave pattern of a two-armed spiral can propagate with uniform angular velocity Ω_p through a disk of gas and stars provided

$$\Omega - \frac{1}{2}\kappa < \Omega_p < \Omega + \frac{1}{2}\kappa \quad (15)$$

locally, where $\Omega(R)$ is the circular angular velocity and $\kappa(R)$ is the epicyclic frequency

$$\kappa^2 = 4\Omega^2 \left(1 + \frac{R}{2\Omega} \frac{d\Omega}{dR} \right) \quad (16)$$

at radius R in the disk. Given the pattern speed Ω_p , equation (15) defines the interval of R in which the density-wave pattern can exist.

Figure 3 shows the dimensionless functions $\tilde{\Omega}(\tilde{R})$, $\tilde{\kappa}(\tilde{R})$ and the resonance frequencies $\tilde{\Omega} \pm \frac{1}{2}\tilde{\kappa}$, where $\tilde{\Omega} = \Omega/(GM^3/a^3)^{1/2}$, $\tilde{\kappa} = \kappa/(GM^3/a^3)^{1/2}$, for the exponential disk. For pattern speeds $\tilde{\Omega}_p > 0.09$, there is no inner Lindblad resonance ($\Omega_p = \Omega - \frac{1}{2}\kappa$).

For the Schmidt (1965) model of the Galaxy, Lin, Yuan, and Shu (1969) find the likely radius for inner Lindblad resonance to be about 4 kpc; they tentatively associate this with the "3-kpc arm." If this association is correct, then features like the 3-kpc arm should be found only in those systems with relatively slow pattern speeds ($\tilde{\Omega}_p < 0.09$), or for which the surface-density distribution in the inner parts is far from exponential (i.e., galaxies with prominent spheroidal components or massive nuclei).

d) *The Mass-Angular Momentum Distribution*

Mestel (1963) has suggested that the angular momentum of each mass element is conserved as a primeval gas cloud contracts to a galactic disk in centrifugal equilibrium. Define the function $\mathfrak{M}(h)$ as the total mass with angular momentum per unit mass less than h . $\mathfrak{M}(h)$ is then invariant during the contraction, and knowledge of this function could provide a useful constraint on understanding how protogalaxies acquired their angular momentum. We now compute this function $\mathfrak{M}(h)$ for the exponential disk with total mass \mathfrak{M} .

The total mass inside radius \tilde{R} is

$$\mathfrak{M}(\tilde{R}) = \mathfrak{M}[1 - \exp(-\tilde{R}) - \tilde{R} \exp(-\tilde{R})], \quad (17)$$

and the angular momentum per unit mass h is

$$h = RV \quad \text{or} \quad \tilde{h} = \tilde{R} \tilde{V}, \quad (18)$$

where $\tilde{h} = h/(GM/a)^{1/2}$ and \tilde{V} is given in equation (12); \tilde{h} is a monotonically increasing function of \tilde{R} . From equations (17) and (18), the total mass $\mathcal{M}(\tilde{h})$ with angular momentum per unit mass less than \tilde{h} can be computed; it is shown by the full curve in Figure 4.

In § IV we discuss the relevance of the angular-momentum properties of the exponential disk to the formation of galaxies.

III. PHOTOMETRIC PROPERTIES OF THE DISK

The purpose of this section is to derive photometric parameters, such as I_0 and α (see eq. [2]), for as many disk galaxies as possible, to see whether these parameters show

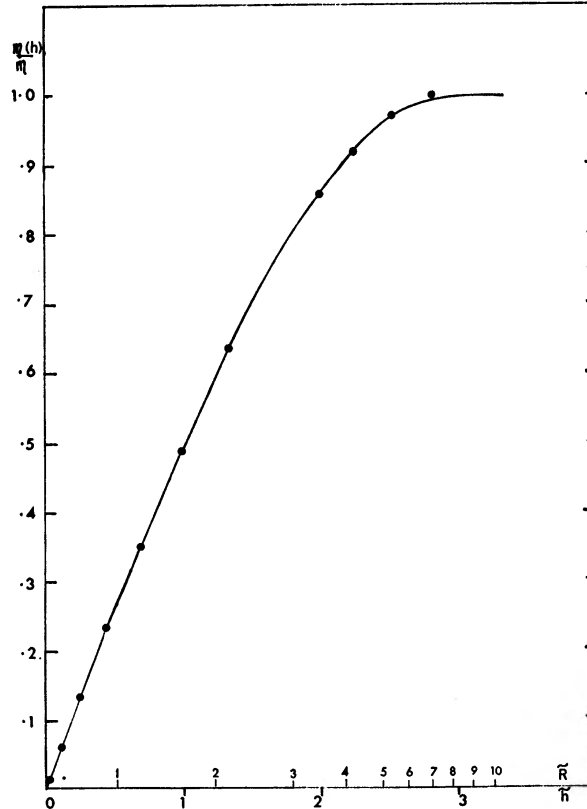


FIG. 4.—The full curve: $\mathcal{M}(\tilde{h})/\mathcal{M}$ for the exponential disk (§ II*d*). \mathcal{M} is the total disk mass. $\tilde{R}(\tilde{h})$ for the disk is also shown. The points are $\mathcal{M}(\tilde{h})/\mathcal{M}$ for the uniformly rotating uniform sphere with $\tilde{h}(\tilde{a}) = \tilde{\Omega}\tilde{a}^2 = 2.80$.

any systematic behavior with morphological type. To derive these parameters, we need galaxies with luminosity profiles that have (a) a well-defined exponential component and (b) a well-defined zero point for the magnitude scale. These two requirements exclude much of the early surface photometry which is often without a zero point, and also exclude the large number of photometric observations which do not go sufficiently faint to define the exponential component unambiguously. It is also necessary to exclude galaxies which are highly inclined to the line of sight (see eq. [20] below).

We find in the literature only thirty-six disk galaxies with luminosity profiles that satisfy the requirements above. The identifications for these galaxies and their classifications in the *Reference Catalogue* (de Vaucouleurs 1964) are given in columns (1) and (2) of Table 1. For most of these galaxies there is only blue-light photometry, so the quantities derived here refer to B -magnitudes: the transformation $B = m_{pg} + 0.1$ is used

TABLE 1
DATA FOR 36 GALAXIES, AND ESTIMATES FOR THE GALAXY

NGC	Class	Source (photom)	Type	$B(0)_c$ \square^{n-2}	Δ (Mpc)	Source (Δ)	α^{-1} (kpc)	$-M_B$	Source (M_B)	k (mag)	$\frac{R_{sph}}{R_{26.5}}$
224	SA(s)b	<u>1</u>	II	21.4	0.69	<u>17,2</u>	4.5	20.3	<u>1</u>	-.20	...
300	SA(s)d	<u>2,4</u>	I	21.8	2.4	<u>2</u>	2.0	18.4	<u>2,4</u>	.05	.11
598	SA(s)cd	<u>5</u>	I	21.4	0.72	<u>17,2</u>	1.6	18.3	<u>5</u>	.05	.16
613	SB(rs)bc	<u>4</u>	I	21.6	15	<u>H</u>	3.7	20.4	<u>4</u>	.50	.36
1291	SB(s)0/a	<u>6</u>	II	19.7	8.0	<u>4</u>	2.5	20.3	<u>4,6</u>	-.65	...
1313	SB(s)d	<u>4,7</u>	I	21.5	4.5	<u>7</u>	1.6	18.7	<u>4,7</u>	.55	.40
1332	S(s)0 ⁻	<u>8</u>	I	22.0	15	<u>H</u>	4.0	19.9	<u>2</u>	.30	.64
1566	SAB(s)bc	<u>4</u>	I	22.1	11.5	<u>2</u>	3.9	20.6	<u>4</u>	1.10	.55
3347	SB(s)ab	<u>4</u>	I	21.435
4267	SBO ⁻	<u>10</u>	II	21.2	11.5	<u>2</u>	1.4	18.7	<u>2</u>	.55	...
4270	SO	<u>11</u>	II	20.0	16	<u>2</u>	0.89	18.1	<u>12</u>	-.30	...
4343	SA(rs)b	<u>11</u>	II	21.6	16	<u>2</u>	0.99	18.0	<u>12</u>	.95	...
4377	SAO ⁻	<u>11</u>	II	20.1	11.5	<u>2</u>	0.61	18.0	<u>12</u>	.50	...
4379	SBO	<u>11</u>	I	21.9	11.5	<u>2</u>	1.0	17.8	<u>12</u>	1.05	.72
4417	SB(s)0	<u>10</u>	II	21.0	11.5	<u>2</u>	1.3	18.3	<u>2</u>	.15	...
4435	SB(s)0 ⁰	<u>11</u>	I	22.0	11.5	<u>2</u>	1.9	19.0	<u>12</u>	.90	.65
4442	SB(s)0 ⁰	<u>10</u>	II	21.5	11.5	<u>2</u>	1.9	18.9	<u>2</u>	.35	...
4459	SA(r)0 ⁺	<u>10</u>	I	21.9	11.5	<u>2</u>	2.4	18.8	<u>2</u>	.15	.51
4476	SA(r:)0 ⁻	<u>11</u>	I	22.0	11.5	<u>2</u>	1.0	17.4	<u>12</u>	.75	.52
4503	SBO ⁻	<u>10</u>	I	21.7	11.5	<u>2</u>	1.5	18.4	<u>2</u>	.50	.33
4526	SAB(s)0 ⁰	<u>10</u>	II	21.2	11.5	<u>2</u>	2.9	19.9	<u>2</u>	.10	...
4578	SO	<u>10</u>	I	21.9	11.5	<u>2</u>	1.6	18.6	<u>12</u>	.80	.24
4694	SB0p	<u>10</u>	I	21.7	11.5	<u>2</u>	1.6	18.4	<u>2</u>	.45	.58
5005	SAB(rs)bc	<u>13</u>	I	21.8	14	<u>13</u>	3.5	20.1	<u>13</u>	.55	.65
5102	SAO ⁻	<u>4</u>	II	19.8	4.0	<u>2</u>	0.86	18.6	<u>4</u>	.10	...
5128	SOp	<u>4</u>	I	21.4	4.0	<u>2</u>	3.9	20.4	<u>4</u>	.20	.42
5236	SAB(s)c	<u>4</u>	II	17.7	4.0	<u>2</u>	1.1	20.5	<u>4</u>	-.65	...
5253	IBmp	<u>4</u>	I	21.2	4.0	<u>2</u>	0.92	18.4	<u>4</u>	1.15	.45
6744	SAB(r)bc	<u>14</u>	II	21.6	4.2	<u>14</u>	2.6	19.1	<u>14</u>	.00	...
6753	SA(r)b	<u>4</u>	I	19.1	30	<u>H</u>	3.1	22.0	<u>4</u>	.00	.38
7424	SAB(rs)od	<u>4</u>	I	22.2	13.2	<u>2</u>	6.1	20.0	<u>4</u>	-.40	.15
7582	SB(s)ab	<u>4</u>	I	21.7	13.2	<u>2</u>	2.2	19.6	<u>4</u>	.95	.42
7793	SA(s)dm	<u>4</u>	II	19.4	2.4	<u>2</u>	0.68	18.2	<u>4</u>	-.20	...
IC 1613	Im	<u>15</u>	I	23.7	0.70	<u>17,2</u>	0.77	14.4	<u>15</u>	-.05	<.35
LMC	SB(s)m	<u>16</u>	I	21.5	0.05	<u>2</u>	1.5	18.1	<u>16</u>	.05	.30
SMC	IB(s)m	<u>16</u>	II	21.6	0.05	<u>2</u>	0.63	16.0	<u>16</u>	-.05	...
Galaxy	SAB(rs)bc:	<u>18</u>	II	17.8:	1.6:	19.9:

Sources:

- | | | | |
|-----|--|------|------------------------|
| (1) | de Vaucouleurs (1958) | (10) | Liller (1960) |
| (2) | de Vaucouleurs (1970) | (11) | Liller (1966) |
| (3) | de Vaucouleurs and Page (1962) | (12) | de Vaucouleurs (1961) |
| (4) | Sersic (1969) | (13) | Bertola (1967) |
| (5) | de Vaucouleurs (1959b) | (14) | de Vaucouleurs (1963c) |
| (6) | de Vaucouleurs (private communication) | (15) | Ables (1968) |
| (7) | de Vaucouleurs (1963a) | (16) | de Vaucouleurs (1960) |
| (8) | Hodge and Webb (1964) | (17) | Sandage (1962) |
| (9) | de Vaucouleurs (1963b) | (18) | Appendix II |

H denotes distance derived from Hubble law with $H = 100 \text{ km sec}^{-1} \text{ Mpc}^{-1}$

where necessary. Apart from this transformation, the zero points used are those given by the observer.

First we distinguish two types of luminosity profile; clear examples of each type are given in Figure 1. Type I (like NGC 4459) has the surface brightness $I(R) \geq I_0 e^{-aR}$ for all observable R . Type II (like NGC 5236) has $I(R) < I_0 e^{-aR}$ in an interval $R_1 < R < R_2$ not far from the center of the system. The Type II profile is almost certainly not an internal-absorption effect; eight of the seventeen S0 galaxies in our sample are of Type II, and for S0 systems the internal absorption is probably very small (Holmberg 1958). Column (3) of Table 1 gives the source of the luminosity profile, and column (4) gives the profile type. For some systems with weak spheroidal components, like M33 (Type I) and NGC 4417 and NGC 4442 (Type II), it is difficult to decide whether the profiles are of Type I or Type II. However, none of the conclusions of this paper depends on the assignment of profile type to these marginal examples.

From equation (2), the luminosity distribution $I(R)$ in the exponential disk is defined by two scales: an intensity scale I_0 and a length scale a^{-1} . The observed $I(R)$ distribution is usually given in B -magnitudes per square second of arc; $B(R)$ is then linear for the exponential disk and is independent of the distance to the galaxy. By extrapolating the exponential component to $R = 0$, the *apparent* intensity scale

$$B(0) = -2.5 \log I_0 + \text{const.} \quad (19)$$

is easily derived. Because we include only those galaxies with well-defined exponential components, the estimated probable error in $B(0)$ is in all cases less than 0.2 mag.

To obtain the *intrinsic* intensity scale for the disk, $B(0)$ must be corrected for the inclination of the galaxy to the line of sight (the optical path through the galaxy increases with inclination) and for galactic absorption. The corrected quantity

$$B(0)_c = B(0) + 2.5 \log \mathfrak{R} - 0.2 \operatorname{cosec} |b^{\text{II}}| \quad (20)$$

is then the intensity scale of the face-on absorption-free luminosity distribution for the exponential disk; it is given in column (5) of Table 1. \mathfrak{R} is the ratio of major to minor diameter for the disk, and is derived from isophotes of the galaxy. The quantity b^{II} is new galactic latitude; the coefficient of the cosecant term comes from de Vaucouleurs and Malik (1969). None of the galaxies has $\log \mathfrak{R} > 0.6$ or $|b^{\text{II}}| < 19^\circ$. No correction has been made for *internal* absorption.

Figure 5 shows $B(0)_c$ against morphological type. This figure contains the main result of this section: *for twenty-eight of the thirty-six galaxies, $B(0)_c$ is nearly constant at $B(0)_c = 21.65 \pm 0.30(\sigma)$ mag per square second of arc along the entire type sequence from S0 to Im, despite a range in absolute magnitude of nearly 5 mag.* (The standard deviation is of the same order as the error in $B(0)_c$ due to uncertainties in deriving $B(0)$.) Seven of the remaining eight systems have $B(0)_c$ more than 1.5 mag brighter than this mean; they include galaxies of early and late types, and their luminosity profiles are drawn from three independent sources. The eighth system is the dwarf irregular of low surface brightness, IC 1613. Before discussing the remarkable result shown in Figure 5, it is necessary to derive the gradient a of the exponential component for these galaxies.

The gradient a in the direction of the major axis can be obtained easily, in angular units, from the slope of the exponential component of the luminosity profile $B(R)$; for nearly all the systems in Table 1, the estimated probable error in a is less than 5 percent. The distance Δ of the galaxy is needed to convert a to linear units. Columns (6) and (7) of Table 1 give Δ and its source; most of the distances are group distances (de Vaucouleurs 1970). Column (8) gives the derived length scale a^{-1} (kpc) for the exponential disk.

Figure 6 shows a^{-1} against morphological type. This figure has two important features: (i) the earlier-type systems (S0 to about Sbc) have any value of a^{-1} between

about 1 and 5 kpc, while the late-type systems have predominantly *low* a^{-1} ($\lesssim 2$ kpc); (ii) five of the seven systems of high surface brightness that are defined in Figure 5 are among the galaxies with the lowest values of a^{-1} ($\lesssim 1$ kpc).

We should expect a strong correlation between the absolute magnitude M_B and the length scale a^{-1} because (i) the disk usually provides most of the blue light in spiral and S0 systems (see below; also see de Vaucouleurs 1958), (ii) the total disk luminosity is

$$L = 2\pi I_0/a^2, \quad (21)$$

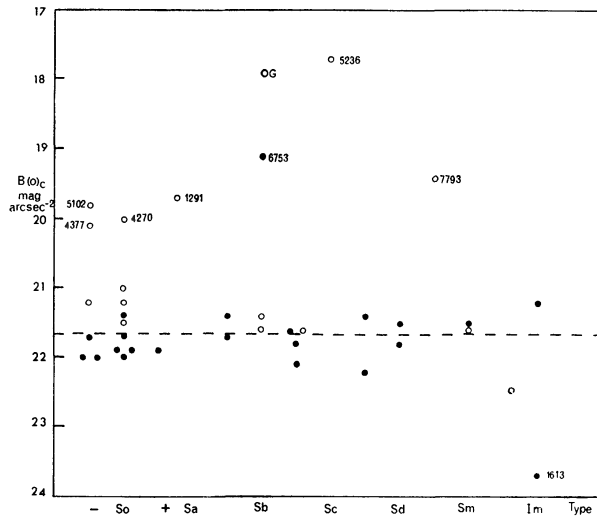


FIG. 5.—Intrinsic distance-independent blue-light luminosity scale $B(0)_c$ for the exponential disks of thirty-six galaxies against their morphological type. Broken line at $B(0)_c = 21.65$ is the mean for twenty-eight galaxies. NGC numbers are shown for the other eight. *G* denotes an estimate for the Galaxy. *Filled circles*, Type I luminosity profile; *open circles*, Type II luminosity profile (see Fig. 1).

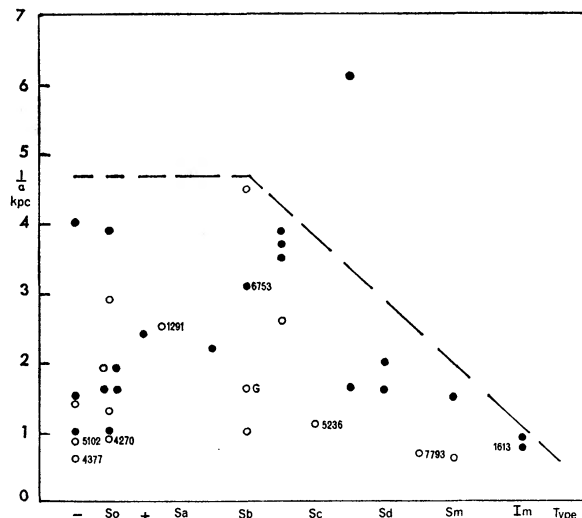


FIG. 6.—Length scale a^{-1} (kpc) for the exponential disks of thirty-six galaxies against their type. NGC numbers are shown for systems defined in Figure 5. *Filled circles*, Type I luminosity profile; *open circles*, Type II luminosity profile (see Fig. 1). *Broken line*, apparent upper envelope. *G* denotes an estimate for the Galaxy.

and (iii) the intensity scale $B(0)_c$ is nearly constant for most spiral systems. In particular, the absolute magnitude for an exponential disk with $B(0)_c = 21.65$ mag per square second of arc (the mean value of $B(0)_c$ given above) is

$$-M_{\text{disk}} = 16.93 + 5 \log (1/a) . \quad (22)$$

Columns (9) and (10) of Table 1 give the absolute magnitude corresponding to the distance Δ and the galactic absorption used in equation (20), and the source of the *total*

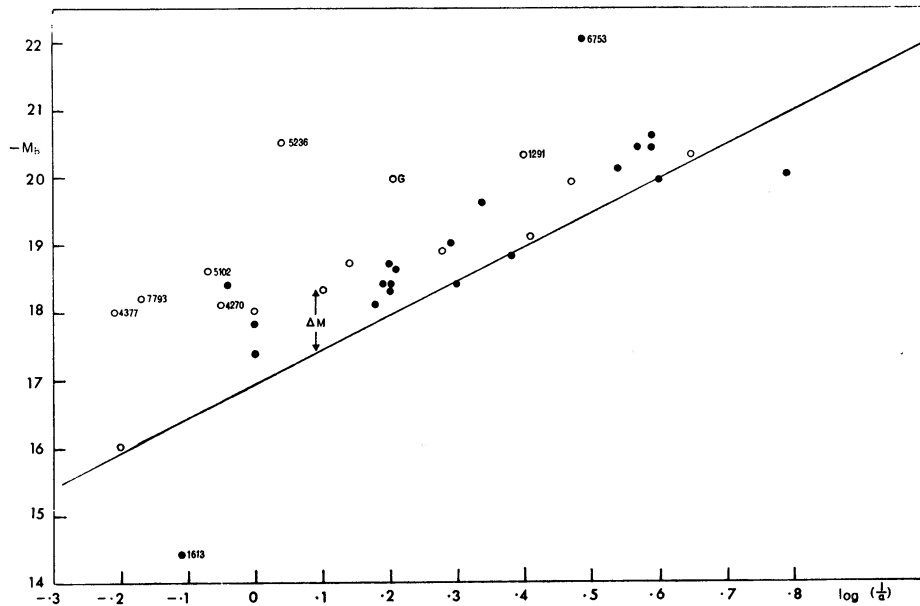


FIG. 7.—Absolute magnitude M_B against the logarithm of the length scale a^{-1} (kpc). Straight line represents $[M_B, \log(a^{-1})]$ -relation for exponential disks with $B(0)_c = 21.65$ mag per square second of arc; see eq. (22). Coding is same as for Fig. 6.

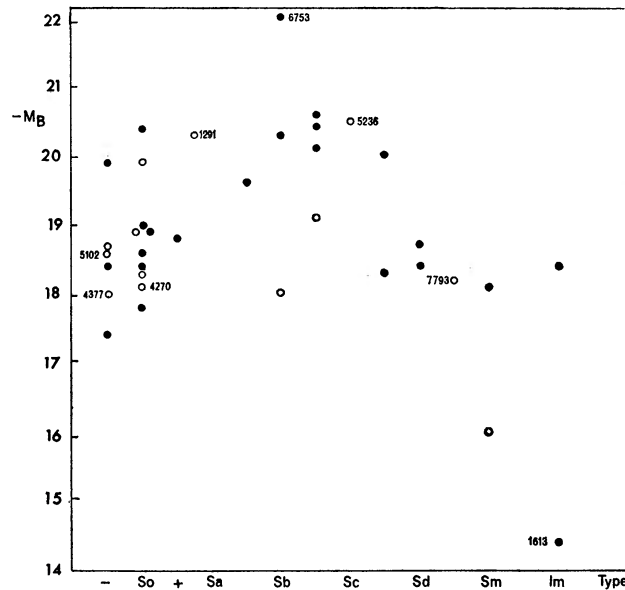


FIG. 8.—Absolute magnitude M_B against morphological type. Coding is same as for Fig. 6.

integrated apparent magnitude used to derive M_B . Figures 7 and 8 show M_B against $\log(1/a)$ and morphological type; the expected correlation of M_B with $\log(1/a)$ is obviously present. Similar correlations (of absolute or apparent magnitude with linear or angular *diameter*) have been found by several authors; see Hubble (1926), de Vaucouleurs (1959c), and Heidmann (1967). These correlations are equivalent to Figure 7 if the diameters are measured consistently at the same surface brightness, because $B(0)_c$ is nearly the same for most spiral systems; diameters are then a measure of the length scale a^{-1} .

We now discuss briefly the relative importance of the spheroidal and exponential components as a function of galaxy type. The straight line representing equations (22) is shown in Figure 7. Because the spheroidal component contributes to the absolute magnitude M_B , most of the points lie above this line, even though $B(0)_c = 21.65$ is the mean value of $B(0)_c$ for all but the labeled points. The deviation ΔM (see Fig. 7) from this line contains information about the contribution of the *spheroidal component* to the total luminosity; it also depends on the difference $[B(0)_c - 21.65]$. Note that ΔM

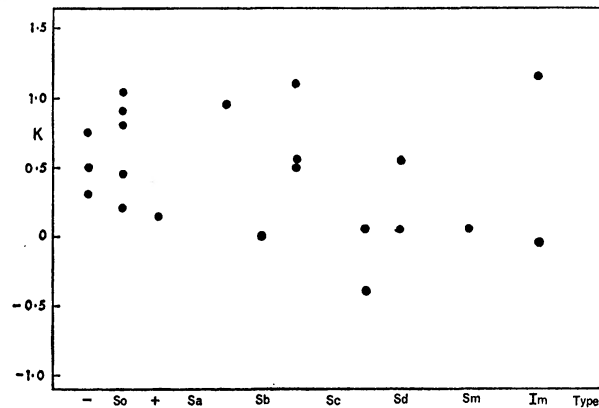


FIG. 9.—The ratio k in magnitudes of the disk luminosity to the total luminosity for systems with Type I luminosity profiles against morphological type.

does *not* depend on the adopted distance Δ , because a change in Δ moves the point parallel to the straight line of equation (22). We can show that the quantity

$$\begin{aligned} k &= \Delta M + [B(0)_c - 21.65] \\ &= -M_B - 5 \log(1/a) + B(0)_c - 38.60 \end{aligned} \quad (23)$$

is the distance-independent ratio (in magnitudes) of the disk luminosity $L = 2\pi I_0/a^2$ (calculated from the observed $B(0)_c$ and a) to the total luminosity of the galaxy (disk + spheroidal component). The ratio k is given in column (11) of Table 1; the error in k , which comes from uncertainties in the total apparent magnitude, a , and $B(0)_c$, is unlikely to exceed 0.3 mag.

Figure 9 shows k against morphological class for the galaxies with Type I luminosity profiles. Type II systems are not shown in Figure 9, because in these the exponential disk obviously does not extend to the center of the system, so k is not a meaningful measure of the spheroidal component luminosity. Figure 9 shows that k is only weakly correlated with morphological type. This correlation is in the usual sense (increasing importance of the spheroidal component for earlier types). In particular, there are *early-type* galaxies in which the spheroidal component contributes only a few percent of the total luminosity.

NGC 7424 (SAB(rs)cd) has $k = -0.4$, which is unphysical. Apart from IC 1613, NGC 7424 is the system in Table 1 with the lowest surface brightness. Because of this,

the photometry does not extend beyond $aR \approx 2.7$. The most likely reason for the negative value of k is then an incorrect value for the integrated apparent magnitude.

The relative importance of the spheroidal component in Type I systems can also be estimated by the ratio of the apparent radius R_{sph} (defined in Fig. 1) of the spheroidal component to the radius of the disk at some consistent surface brightness. Column (12) of Table 1 gives the ratio $R_{\text{sph}}/R_{26.5}$, where $R_{26.5}$ is the radius of the disk at $B = 26.5$ mag per square second of arc (corrected for the inclination of the galaxy). Figure 10 shows that this ratio is only weakly correlated with morphological type. The ratio $R_{\text{sph}}/R_{26.5}$ increases from late to early type; its lowest values are for spirals like M33 and NGC 300. Figure 10 also shows that in the range defined by the Sa–Sm spirals, *the S0 galaxies can have any but the lowest values of $R_{\text{sph}}/R_{26.5}$* . This feature is probably important for understanding the evolution of spiral systems, and it is discussed at length by Sandage *et al.* (1970).

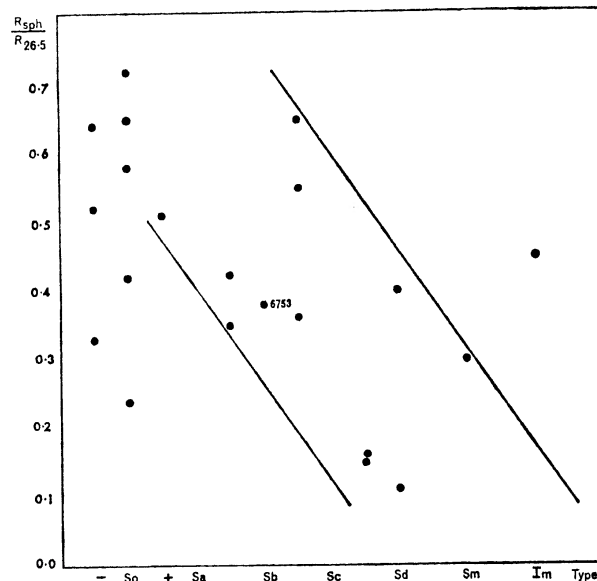


FIG. 10.—The ratio $R_{\text{sph}}/R_{26.5}$ of apparent radius of the spheroidal component (see Fig. 1) to the disk radius at $B = 26.5$ mag per square second of arc (face-on), for galaxies with Type I luminosity profiles. Straight lines represent the apparent envelope for Sa–Im systems.

To summarize this section, we find the following:

- i) Twenty-eight of the thirty-six galaxies have approximately the same value of the disk luminosity scale $B(0)_c = 21.65 \pm 0.30$ (σ) mag per square second of arc (Fig. 5). This explains the observed correlation between apparent magnitude and diameter for spiral systems.
- ii) S0 to Sbc systems have any value of the disk length scale a^{-1} between about 1 and 5 kpc, while the later-type systems have predominantly low values of a^{-1} ($\lesssim 2$ kpc).
- iii) The relative brightness and size of the spheroidal and disk components are only weakly correlated with morphological type. In particular, there exist S0 systems with dominant and with weak spheroidal components.

IV. DISCUSSION

a) *The Uniformity of $B(0)_c$*

In § I we inferred that the disk luminosity distribution $I = I_0 e^{-aR}$ implies a surface density distribution $\mu = \mu_0 e^{-aR}$. This followed from the assumption that a radially uni-

form $B - V$ color in the disk means a radially uniform mass/luminosity ratio. The main results of § III is that I_0 is approximately constant for twenty-eight of the thirty-six galaxies. Can we infer from this result that the *surface-density* scale μ_0 for these galaxies is also approximately constant?

The sample of galaxies with $B(0)_c \approx 21.65$ includes systems with integrated colors in the range $0.5 < B - V < 1.0$. For the few galaxies with detailed color distributions, $B - V$ in the disk is similar to the integrated $B - V$ (e.g., M33 [$B - V = 0.5$]; M31 [$B - V = 0.9$]; NGC 1332 [$B - V = 1.0$]). This color range for the disks makes it difficult to establish properly whether μ_0 is as uniform as is $B(0)_c$, because there is almost no direct information about the dependence of the *disk's* mass/luminosity ratio on color (or type; see Holmberg 1958). However, Roberts (1969) has shown that, contrary to previous belief, the mean ratio of total mass to blue light for spiral galaxies of a given type is approximately the same for all types, although the scatter in \mathcal{M}/L at a given type is fairly large. Because the disk color and the integrated color appear to be similar, and because the disk provides a substantial fraction of the integrated blue light, we tentatively infer that the ratio of mass to blue light for the *disk* is approximately the same (at least within a factor of about 2) from galaxy to galaxy. The surface-density scale μ_0 is then also the same from galaxy to galaxy, within a similar factor, although the *masses* of the galaxies in the sample of twenty-eight have a range of about 5 mag (or a factor of 100). We emphasize that this conclusion is rather weak, mainly because the mass/luminosity ratios in the disk are difficult to determine directly.

If it is correct that μ_0 is approximately constant, then there is an important consequence. The mass of the exponential disk is $\mathcal{M}_D = 2\pi\mu_0/a^2$, and the total angular momentum for the disk in centrifugal equilibrium (§ IIb) is $\mathcal{S}_D = 1.109 (G\mathcal{M}_D^3/a)^{1/2}$. It then follows that

$$\mathcal{S}_D \propto \mathcal{M}_D^{7/4}. \quad (24)$$

Because most of the angular momentum of spiral and S0 systems lies in the disk, and because the mass of the disk is probably a large fraction of the total mass, we should expect the total mass \mathcal{M}_T and angular momentum \mathcal{S}_T for most of these systems to follow fairly closely the law

$$\mathcal{S}_T \propto \mathcal{M}_T^{7/4}. \quad (25)$$

This result would hold on dimensional grounds for *any* surface-density distribution $\mu = \mu(R; \mu_0, L)$, where L is a *single* length scale, if μ_0 is constant from system to system. Conversely, because \mathcal{S}_T and \mathcal{M}_T are probably endowed properties of a protogalaxy which are conserved as it collapses to form a galaxy, the apparent constancy of μ_0 for most spirals would be explained if we understood why the galactic disks have only one length scale and if we knew that the distribution of masses and angular momenta in protoclouds followed the law $\mathcal{S} \propto \mathcal{M}^{7/4}$.

Unfortunately, there is an essential difficulty in deriving observationally the $\mathcal{S}(\mathcal{M})$ law for disk galaxies. For example, Takase and Kinoshita (1967) looked for a relation $\mathcal{S} \propto \mathcal{M}^p$ in a sample of sixteen spiral systems with known rotation curves. They fitted Brandt functions (Brandt and Belton 1962)

$$V = AR/(1 + B^n R^n)^{3/2n} \quad (26)$$

to the observed rotation curves $V(R)$. The total mass and angular momentum of the disks associated with these velocity laws are

$$\mathcal{M} = (A^2/B^3)c_1, \quad (27)$$

$$\mathcal{S} = (A^3/B^5)c_2, \quad (28)$$

where c_1, c_2 , are slowly varying functions of n . From the values of A and B that they derived, and from equations (27) and (28), Takase and Kinoshita showed that spiral systems appear to follow very closely the law

$$\log \mathfrak{S} = \text{const.} + \frac{7}{4} \log \mathfrak{M} \quad (29)$$

which is exactly the law of equation (25) derived photometrically for the exponential disks.

This result is not the striking kinematical verification of the photometrically predicted mass-angular momentum relation that it appears to be. The photometric prediction of equation (25) follows from the rotation curve of equation (10); this rotation curve has two parameters, μ_0 and a , and equation (25) is a consequence of the apparent constancy of μ_0 for most galaxies. \mathfrak{M} and \mathfrak{S} then depend on only *one* parameter, a . On the other hand, from equations (27) and (28), \mathfrak{M} and \mathfrak{S} for the Brandt-function disks are *two*-parameter (A and B) quantities. The law $\mathfrak{S} \propto \mathfrak{M}^{7/4}$ then implies $A^2 \propto B$; however even though Takase and Kinoshita find $\log \mathfrak{S} = \text{const.} + \frac{7}{4} \log \mathfrak{M}$, it is clear from their Table 2 that A^2 is *not* proportional to B . This apparent inconsistency comes about because, from equations (27) and (28),

$$\log \mathfrak{S} - \theta \log \mathfrak{M} = (3 - 2\theta) \log A + (3\theta - 5) \log B + c_3, \quad (30)$$

where θ is a number and c_3 is a slowly varying function of n . For the sixteen galaxies in the sample, $0 < \log A < 1.2$ and $-0.4 < \log B < 0.8$. In the vicinity of $\theta = \frac{7}{4}$ the coefficients $(3 - 2\theta)$ and $(3\theta - 5)$ in equation (30) are both small and are of opposite sign; $\log \mathfrak{S} - \frac{7}{4} \log \mathfrak{M}$ then appears to be approximately constant from galaxy to galaxy, whether or not $A^2 \propto B$. As this result holds for *any* rotation curve with one length scale and one time (or mass) scale, the search for a law $\log \mathfrak{S} = \theta \log \mathfrak{M} + \text{const.}$ by fitting two-parameter rotation curves to observed rotation curves will always yield $\theta \approx \frac{7}{4}$, *whether or not $\mathfrak{S} \propto \mathfrak{M}^{7/4}$ is really true* (see also Brosche 1963). Because of this difficulty, the mass-angular momentum relation for spiral galaxies remains uncertain.

It is worth comparing our inference that μ_0 is approximately constant for most disk galaxies with Fish's (1964) results for ellipticals.¹ He finds that the observed masses \mathfrak{M} and potential energies Ψ follow a law $\Psi \propto \mathfrak{M}^x$, where the exponent x lies between 1.3 and 1.8 and is probably about 1.5. Because $\Psi \propto \mathfrak{M}^2/R$, where R is a length scale, it follows from $\Psi \propto \mathfrak{M}^{1.5}$ that $\mathfrak{M} \propto R^2$, so the mean surface density is approximately constant from galaxy to galaxy. Although these two results are similar in that the surface-density scales appear to be uniform both for ellipticals and for disk galaxies, the physical reasons for these two results are probably quite different. For the ellipticals, Fish shows that the $\Psi \propto \mathfrak{M}^{1.5}$ law would follow if the collapse of protoellipticals were halted when their optical depth to free-electron scattering became sufficiently high; i.e., the $\Psi \propto \mathfrak{M}^{1.5}$ law is established late in the collapse phase. For the disk systems, we show that the constancy of μ_0 would result from the law $\mathfrak{S} \propto \mathfrak{M}^{7/4}$; because \mathfrak{S} and \mathfrak{M} are presumably conserved quantities, it seems likely that *this* law is established very early in the history of the protogalaxies.

b) The Mass-Angular Momentum Distribution

In § II*d* we derived the mass-angular momentum distribution $\mathfrak{M}(h)$ for the exponential disk in centrifugal equilibrium; it is shown by the full curve in Figure 4. Mestel (1963) has suggested that $\mathfrak{M}(h)$ is invariant during the collapse of a protocloud to form a galaxy. If this is correct, then because the exponential disk is such a general property of the disk galaxies, it follows that *all* protoclouds destined to be SO or spiral galaxies have a similar $\mathfrak{M}(h)$ (in a dimensionless sense), at least for the higher values of h cor-

¹ I am grateful to Dr. Alar Toomre for suggesting this comparison.

responding to the exponential disk. Mechanisms for the acquisition of angular momentum by protogalaxies should then predict this $\mathfrak{M}(h)$. Alternatively, if $\mathfrak{M}(h)$ is not invariant during the collapse, then there must exist a very efficient mechanism which establishes the characteristic $\mathfrak{M}(h)$ for the disk systems as they form.

Crampin and Hoyle (1964) show that the angular-momentum distribution in the outer parts of several spiral systems is very similar to the distribution for a uniformly rotating uniform spheroid. We now compare $\mathfrak{M}(h)$ for the exponential disk of gradient a and total mass \mathfrak{M} with the $\mathfrak{M}(h)$ for the disk D of surface density

$$\begin{aligned} \mu(R) &= \mu_0(1 - R^2/a^2)^{1/2}, & R \leq a, \\ &= 0, & R > a, \end{aligned} \quad (31)$$

uniform angular velocity Ω , and the same total mass \mathfrak{M} as the exponential disk. This *disk* D has exactly the same $\mathfrak{M}(h)$ as a uniformly rotating uniform *sphere* with the same \mathfrak{M} , Ω , and radius a ; it has

$$\mathfrak{M}(\tilde{h})/\mathfrak{M} = 1 - [1 - (\tilde{h}/\tilde{\Omega}\tilde{a}^2)]^{3/2}, \quad (32)$$

where, again, $\tilde{h} = h/(G\mathfrak{M}/a)^{1/2}$ and $\tilde{a} = aa$. (We are using the same length scale a^{-1} to write $\mathfrak{M}(h)$ in dimensionless form for both the exponential disk and the disk D .) It turns out that for $\tilde{\Omega}\tilde{a}^2 \approx 2.80$, $\mathfrak{M}(h)$ for the disk D is almost identical with the $\mathfrak{M}(h)$ for the exponential disk with the same mass \mathfrak{M} . Only for the outer part of the exponential disk ($\tilde{R} > 6$), which contains less than 0.2 of the total mass and 0.05 of the total angular momentum, do the two functions $\mathfrak{M}(h)$ differ significantly (see Fig. 4).

This means that to each exponential disk in centrifugal equilibrium with mass \mathfrak{M} and gradient a there corresponds a family of uniformly rotating disks D with the same mass \mathfrak{M} and with $\tilde{\Omega}\tilde{a}^2 = \tilde{h}(\tilde{a}) \approx 2.80$, such that $\mathfrak{M}(h)$ for the exponential disk and for the disks D are almost identical. In particular, one member of each such family of disks D is also in centrifugal equilibrium; it satisfies

$$\tilde{\Omega}^2\tilde{a}^3 = 3\pi/4, \quad (33)$$

and so has $\tilde{a} = 3.33$ and $\tilde{\Omega} = 0.253$ (cf. Fig. 3).

It may be worth emphasizing here that not all zero-thickness disks in centrifugal equilibrium have $\mathfrak{M}(h)$ similar to that for the sphere. For example, for the sequence of Brandt-function disks (eq. [26]) with integral n , it is easy to show that $\mathfrak{M}(h)$ is clearly different from the uniform sphere $\mathfrak{M}(h)$ for all n .

Almost all spirals show central mass concentration above that of the exponential disk. Because h increases monotonically with R , this corresponds to an excess of low- h matter in the protogalaxy (if Mestel's hypothesis is correct) above the requirements of the disk. The amount of this excess low- h matter presumably determines the mass of the low- h spheroidal component (Sandage *et al.* 1970).

c) The Two Types of Luminosity Profile

Figure 1 shows the two types of luminosity profile; they are defined in § III. The Type I profile appears to be the sum of the exponential disk $I(R)$ and the much steeper $I(R)$ corresponding to the spheroidal component; there is no reason to believe that the exponential disk does not extend in to $R = 0$. However, for galaxies with Type II profiles, the exponential disk obviously does not extend to the center.

As we pointed out in § III, it is unlikely that the Type II profile is the result of internal absorption. It probably corresponds to a real deficiency, compared with the exponential disk, of luminous matter with angular momentum per unit mass in the range $h(R_1) < h < h(R_2)$.

There appears to be a subgroup of the Type II galaxies which have very bright disk

luminosity scales $B(0)_c$ and rather small length scales α^{-1} . Their luminosity profiles are all very clear examples of the Type II profile. $B(0)_c$ is shown in Figure 5; if Innanen's (1966) model gives a good representation of the outer parts ($R > 10$ kpc) of our Galaxy, then it belongs to this subgroup (see Appendix B). Of the seven galaxies with $B(0)_c$ much brighter than the mean value $B(0)_c \approx 21.65$, six are Type II; the remaining one is NGC 6753, which is probably an extremely luminous spiral ($M_B \approx -22$). For five of these six systems, Figure 6 shows that the length scale α^{-1} for the disk is less than about 1 kpc, which is of the same order as α^{-1} for the dwarf irregular IC 1613. The high $B(0)_c$ and low α^{-1} for this subgroup combine to give normal absolute magnitudes and normal apparent diameters. We note, however, that eight of the fourteen Type II galaxies in Table 1 have normal $B(0)_c$ ($\approx 21.65 \pm 0.30$) and normal α^{-1} for their absolute magnitudes.

It is worth pointing out that for the three true spiral (rather than S0) galaxies in which the Type II characteristic is most prominent (M31, M83, and NGC 7793), the exponential disk begins *outside* the main region of spiral-arm activity. For example, in M83 (see Sandage 1961), the really bright spiral structures lies between R_1 and R_2 (see Fig. 1); the disk is present and is very well defined for $R > R_2$. We note that M83 and the Galaxy may have fairly similar photometric properties: $(M_B, B(0)_c, \alpha^{-1}) = (-20.5, 17.7, 1.1$ kpc) for M83 and $(-20, 17.8, 1.6$ kpc) for the Galaxy (according to the estimates made in Appendix B).

Because the formation of the exponential disk is not understood, we can only speculate on the origin of the Type II phenomenon. If $\mathfrak{M}(h)$ is strictly invariant throughout the collapse phase, then the deficiency of matter with $h(R_1) < h < h(R_2)$ for Type II galaxies is inherent in the protocloud. If $\mathfrak{M}(h)$ is not invariant, then only the total mass \mathfrak{M} and angular momentum \mathfrak{S} are conserved during the collapse. Assume that all the angular momentum goes into the disk. Then because the disk mass $\mathfrak{M}_D = \text{const.} \times \mathfrak{S}^{4/7}$ for most spirals, the mass of the spheroidal component is $\mathfrak{M}_S = \mathfrak{M} - \text{const.} \times \mathfrak{S}^{4/7}$. It seems plausible that a Type I galaxy forms if $\mathfrak{M}_S > 0$. Now say $\mathfrak{M}_S < 0$. This means that the protogalaxy has more angular momentum than its mass \mathfrak{M} can accommodate in an exponential disk. It is again plausible that the disk adjusts to minimize the amount of matter with low angular momentum, and so forms a Type II configuration. In particular, we could expect most of the galaxies with very bright $B(0)_c$ and low α^{-1} to be of Type II; because $\mathfrak{S} \propto (\mathfrak{M}_D^3/\alpha)^{1/2}$ (§ IIb), a protocloud which forms a disk of lower α^{-1} will have more difficulty in accommodating its angular momentum in a purely exponential disk.

d) The Dwarf Irregulars

There is one dwarf irregular, IC 1613, among the thirty-six galaxies of Table 1. Its value of $B(0)_c$ is 23.7, about 2 mag fainter than the mean value for the sequence of galaxies with $\langle B(0)_c \rangle = 21.65$ in Figure 5. Its length scale α^{-1} is of the same order as α^{-1} for the Magellanic Clouds, giving an absolute magnitude $M_B = -14.4$. While the SMC ($M_B = -16.0$) appears to be a faint member of the $\langle B(0)_c \rangle = 21.65$ sequence, the disk of IC 1613 obviously does not belong to this sequence. Photometry of faint Magellanic systems and dwarf irregulars could determine whether there is a minimum absolute magnitude for the formation of disks belonging to the $\langle B(0)_c \rangle = 21.65$ sequence. This would be of some interest for the theory of galaxy formation. We note, however, that the very small irregular galaxy GR 8 (Hodge 1967) has a roughly exponential luminosity profile with $B(0)_c \approx 21.7$. The absolute magnitude of this system is uncertain; it is almost certainly fainter than $M_B = -13$, and may be as faint as $M_B = -8$.

e) Why an Exponential Disk?

According to Eggen, Lynden-Bell, and Sandage (1962), the galactic disk formed from matter which had remained gaseous during the rapid-collapse phase. This matter lost

its random kinetic energy through inelastic encounters of gas clouds and, conserving its angular momentum, settled to a disk, approximately in centrifugal equilibrium. Because the disk is so flat, and because it is difficult to dissipate the energy of random *stellar* motions perpendicular to the galactic plane, it seems very likely that the settling to the disk was virtually complete before the main burst of star formation in the disk began; this burst presumably formed the old disk population (stars as old as or older than NGC 188). Why is the disk, which results from this process, exponential? We cannot yet answer this; all we can do is to make the following points.

i) The exponential disk is not just an old disk property. It seems to involve the complete stellar content. For example, in M33 (de Vaucouleurs 1959*b*), which is an almost pure exponential disk, the ultraviolet luminosity distribution $U(R)$ is exponential with the same gradient a as $B(R)$ and the visual $V(R)$. Since the young Population I presumably contributes significantly to $U(R)$, this population is also exponentially distributed. The gas associated with the young Population I is probably the remains of gas left over after the old disk population formed (see Sandage *et al.* 1970). This suggests that the exponential disk was defined during the settling phase of the disk, *before* significant star formation in the disk began.

ii) Figures 8 and 9 show that for most morphological types there is a considerable range in the relative brightness and size of the spheroidal and disk components. This suggests that the process leading to the exponential disk does not depend much on the mass of the spheroidal component, which presumably fragmented and relaxed before and during the time in which the disk was settling.

iii) The mass-angular momentum distribution $\mathcal{M}(h)$ does not alone define the exponential disk. In § IV*b* we pointed out that to each exponential disk there corresponds a disk D with almost identical $\mathcal{M}(h)$, derivable from a uniform, uniformly rotating sphere (eq. [31]), and which is also in centrifugal equilibrium. However, given the invariance of $\mathcal{M}(h)$ during the collapse phase, it is unlikely that the disk D should be the end product; Hunter (1963) has shown that this disk, in centrifugal equilibrium, is unstable. Nevertheless, there may be other centrifugal-equilibrium states, all with nearly the same $\mathcal{M}(h)$, between the exponential disk and the disk of equation (31), and some of these may be stable. In particular, it is important to find out whether the exponential disk itself is the most stable of these states.

Toomre (1964) points out that a differentially rotating disk of stars is unstable to axisymmetric disturbances, unless the radial component σ_R of the velocity dispersion exceeds some critical value. He suggests that the action of these instabilities may be to increase σ_R preferentially over σ_Z (the component perpendicular to the galactic plane) until the disk is stabilized; this would explain the observed anisotropic velocity dispersion for most stars in the solar neighborhood. These instabilities could be important as a process capable of defining the exponential nature of the disk *after* most of the disk stars had formed.

f) Conclusion

The main problems pointed out in this paper are: (i) Why are the disks of spiral and S0 systems exponential? (ii) Why is the surface-brightness scale for these disks approximately the same for about three-quarters of the sample, despite the great range in absolute magnitude?

I am very grateful to Dr. A. Sandage for discussion of this problem and for reading the manuscript, and to Dr. G. de Vaucouleurs for his advice. I am also most grateful to Dr. Alar Toomre for much constructive criticism on the presentation and content of this paper.

APPENDIX A

COMPARISON OF OBSERVED AND PREDICTED ROTATION CURVES

There are a few galaxies (only the LMC, SMC, M33, and NGC 300) which have measured rotation curves and surface photometry, and which have weak spheroidal components; the gravitational field is then dominated by the exponential disk over most of the galaxy, so the rotation curve of equation (12) should be appropriate.

From equation (12), the rotational velocity has its maximum at $R = R_T = 2.151/a$, where a is the *photometrically* determined gradient. Here we compare the observed and photometrically predicted values of R_T for these four galaxies. The maximum rotational velocity from equation (12) is $V(R_T) = 0.623(GM/a)^{1/2}$; its value cannot be predicted from the photometry because the mass is not known independently.

a) *Large Magellanic Cloud*

Carrick and Freeman (1970) have derived the velocity field for the LMC from 21-cm data given by McGee and Milton (1966). The rotation curve of equation (12), with $a = 0.010$ per minute of arc (de Vaucouleurs 1960) and $V_{\max} = 80 \text{ km sec}^{-1}$, fits the observed rotation curve within the observational errors.

b) *Small Magellanic Cloud*

Hindman (1967) finds that the H I rotation curve has V_{\max} at $R \approx 2''$ (along the major axis). For $a = 0.023$ per minute of arc (de Vaucouleurs 1960), the theoretical $R_T = 1''.6$, which is within the observational uncertainty.

c) *NGC 300*

Shobbrook and Robinson (1967) find the H I linear dimensions of this system to be about twice the optical photometric dimensions. The theoretical R_T for $a = 0.35$ per minute of arc (de Vaucouleurs and Page 1962) is $6'$. The H I rotation curve has V_{\max} at $R \approx 15'$, which also happens to be the photometric outer edge of the system. If the H I rotation curve is correct, then there must be undetected matter beyond the optical extent of NGC 300; its mass must be at least of the same order as the mass of the detected galaxy. There is no optical rotation data for NGC 300.

d) *M33*

For $a = 0.13$ per minute of arc (de Vaucouleurs 1959b), the theoretical $R_T = 17'$. Optical velocity data by Carranza *et al.* (1968) show a complex velocity field and do not define a unique rotation curve. The rotation curve derived by Mayall and Aller (1942) from velocities of H II regions has R_T at $17'$. Brandt's (1965) optical velocities combined with low-resolution 21-cm velocities have $R_T \approx 25'$; this is consistent with the 21-cm data given by Burke, Turner, and Tuve (1963). As in NGC 300, the value of R_T is of the same order as the optical semimajor axis $a \approx 35'$ (de Vaucouleurs 1959b).

For two of four systems with weak spheroidal components, the LMC and the SMC, the turnover radii of the rotation curves predicted from the photometrically derived gradients a appear to be consistent with those observed. For NGC 300 and M33, the 21-cm data give turnover points near the photometric outer edges of these systems. These data have relatively low spatial resolution; if they are correct, then there must be in these galaxies additional matter which is undetected, either optically or at 21 cm. Its mass must be at least as large as the mass of the detected galaxy, and its distribution must be quite different from the exponential distribution which holds for the optical galaxy.

APPENDIX B

PHOTOMETRIC PARAMETERS FOR OUR GALAXY

Several authors have constructed mass-distribution models for the Galaxy: these models reproduce the galactic rotation curve, the observed local total density, and some features of the

stellar-density distribution in the Galaxy. From the surface-density distribution for these models, we can make rough estimates of photometric parameters ($B(0)_c$, α^{-1} , M_B) for the galactic disk. These estimates are rough because the mass/luminosity ratio is uncertain and because the outer part of the disk determines the intensity scale $B(0)_c$ and the length scale α^{-1} ; the models are necessarily unreliable in this outer part ($R \gtrsim 10$ kpc) because there is little direct information about the circular-velocity field or the stellar-density distribution for $R \gtrsim 10$ kpc.

Figure 11 shows the surface-density distribution $\mu(R)$ for Innanen's (1966) model; μ is in solar masses per square parsec. According to this model the Galaxy has a Type II profile, with

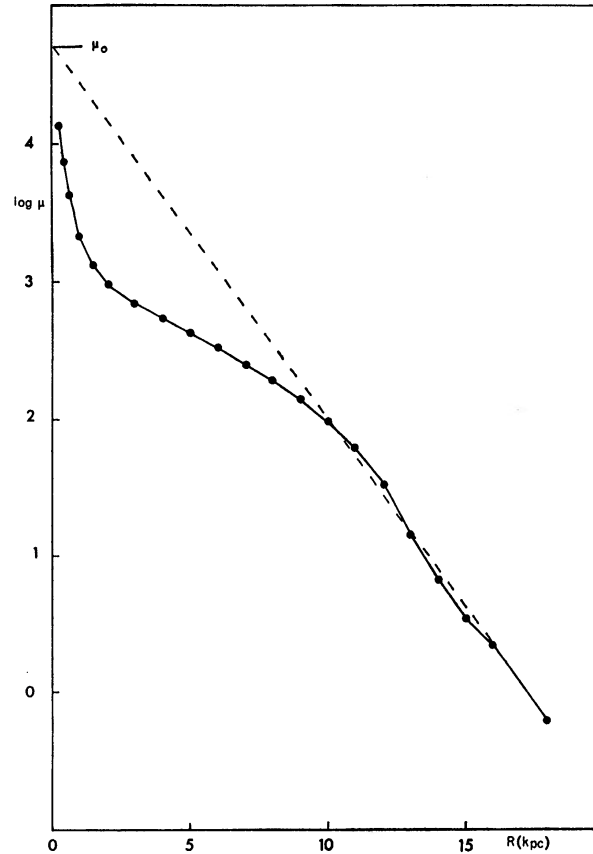


FIG. 11.—Surface-density distribution $\mu(R)$ for the Galaxy, according to Innanen (1966), where μ is in units of $M_{\odot} \text{pc}^{-2}$. Broken line shows the estimated slope of the exponential disk, and μ_0 is the estimated surface-density scale for the disk.

$\mu(R)$ approximately exponential for $R > 10$ kpc. The length scale $\alpha^{-1} \approx 1.6$ kpc, and the surface-density scale μ_0 has $\log \mu_0 = 4.7$. The mass/luminosity ratio \mathfrak{M}/L is not known; we adopt $\mathfrak{M}/L = 10$ as a reasonable value (cf. M31, de Vaucouleurs 1959*b*). $\log \mu_0 = 4.7$ then corresponds to $B(0)_c = 17.8$ mag. As a check, Seares (1920) estimates $V = 23$ mag per square second of arc for the surface brightness at the Sun, which corresponds to $B \approx 24$ mag per square second of arc if $B - V$ has the same value (≈ 1.0) as in M31. The model gives the surface brightness at the Sun ($R = 10$ kpc) as $B = 24.5$ mag per square second of arc, which is in reasonable agreement.

Innanen (1966) gives the total galactic mass as $1.3 \times 10^{11} M_{\odot}$; for the adopted $\mathfrak{M}/L = 10$, the absolute magnitude of the Galaxy is -19.9 . As pointed out in § IV*c*, the Galaxy and NGC 5236 may have rather similar photometric properties. (The morphological type for NGC 5236, from Table 1, is SAB(s)c; according to de Vaucouleurs [1969], the Galaxy has type SAB(rs)bc.) However, we must emphasize again the uncertainty of the photometric parameters derived above for the Galaxy.

REFERENCES

- Ables, H. D. 1968, unpublished dissertation, University of Texas.
- Bertola, F. 1967, *Asiago Contr.*, No. 194.
- Brandt, J. C. 1965, *M.N.R.A.S.*, **129**, 309.
- Brandt, J. C., and Belton, M. J. S. 1962, *Ap. J.*, **136**, 352.
- Brosche, P. 1963, *Zs. f. Ap.*, **57**, 143.
- Burke, B. F., Turner, K. C., and Tuve, M. A. 1963, *Carnegie Inst. Washington Yrb.*, **62**, 289.
- Carranza, G., Courtes, G., Georgelin, Y., Monnet, G., and Pourcelot, A. 1968, *Ann. d'ap.*, **31**, 63.
- Carrick, D. W., and Freeman, K. C. 1970 (in preparation).
- Crampin, D. J., and Hoyle, F. 1964, *Ap. J.*, **140**, 99.
- Eggen, O. J., Lynden-Bell, D., and Sandage, A. 1962, *Ap. J.*, **136**, 748.
- Fish, R. A. 1964, *Ap. J.*, **139**, 284.
- Gradshteyn, I. S., and Ryzhik, I. M. 1965, *Tables of Integrals, Series and Products* (New York: Academic Press).
- Heidmann, J. 1967, *C.R.*, **265**, 866.
- Hindman, J. V. 1967, *Australian J. Phys.*, **20**, 147.
- Hodge, P. W. 1967, *Ap. J.*, **148**, 719.
- Hodge, P. W., and Webb, C. J. 1964, *Ap. J.*, **140**, 681.
- Holmberg, E. 1958, *Lund. Medd.*, Ser. 2, No. 136.
- Hubble, E. 1926, *Ap. J.*, **64**, 321.
- Hunter, C. 1963, *M.N.R.A.S.*, **126**, 299.
- Innanen, K. A. 1966, *Zs. f. Ap.*, **64**, 158.
- King, I. 1966, *A.J.*, **71**, 64.
- Liller, M. H. 1960, *Ap. J.*, **132**, 306.
- . 1966, *ibid.*, **146**, 28.
- Lin, C. C., and Shu, F. 1966, *Proc. Nat. Acad. Sci.*, **55**, 229.
- Lin, C. C., Yuan, C., and Shu, F. H. 1969, *Ap. J.*, **155**, 721.
- Lynden-Bell, D. 1967, *M.N.R.A.S.*, **136**, 101.
- McGee, R. X., and Milton, J. A. 1966, *Australian J. Phys. Ap. Suppl.*, No. 2.
- Mayall, N. U., and Aller, L. H. 1942, *Ap. J.*, **95**, 5.
- Mestel, L. 1963, *M.N.R.A.S.*, **126**, 553.
- Roberts, M. S. 1969, *A.J.*, **74**, 859.
- Sandage, A. 1961, *The Hubble Atlas* (Washington: Carnegie Institution of Washington).
- . 1962, *Problems of Extragalactic Research*, ed. G. C. McVittie (New York: Macmillan Co.), p. 366.
- Sandage, A., Freeman, K. C., and Stokes, N. R. 1970, *Ap. J.*, **160**, 831.
- Schmidt, M. 1965, *Stars and Stellar Systems*, **5**, ed. A. Blaauw and M. Schmidt (Chicago: University of Chicago Press), chap. 22.
- Schwarzschild, M. 1954, *A.J.*, **59**, 273.
- Seares, F. H. 1920, *Ap. J.*, **52**, 162.
- Sersic, J. 1969, *Galaxias Australes* (Cordoba: Universidad Nacional de Cordoba).
- Shobbrook, R. R., and Robinson, B. J. 1967, *Australian J. Phys.*, **20**, 131.
- Takase, B. 1967, *Pub. Astr. Soc. Japan*, **19**, 427.
- Takase, B., and Kinoshita, H. 1967, *Pub. Astr. Soc. Japan*, **19**, 409.
- Toomre, A. 1963, *Ap. J.*, **138**, 385.
- . 1964, *ibid.*, **139**, 1217.
- Vaucouleurs, G. de. 1958, *Ap. J.*, **128**, 465.
- . 1959a, *Hdb. d. Phys.*, **53**, 311.
- . 1959b, *Ap. J.*, **130**, 728.
- . 1959c, *Ann. Obs. Houga*, **2**, 5.
- . 1960, *Ap. J.*, **131**, 574.
- . 1961, *Ap. J. Suppl.*, **6**, 213.
- . 1963a, *Ap. J.*, **137**, 720.
- . 1963b, *Ap. J. Suppl.*, **8**, 31.
- . 1963c, *Ap. J.*, **138**, 934.
- . 1964, *A Reference Catalogue of Bright Galaxies* (Austin: University of Texas Press).
- . 1969, *I.A.U. Symposium No. 38* (in press).
- . 1970, *Stars and Stellar Systems*, Vol. 9, ed. A. and M. Sandage (Chicago: University of Chicago Press), chap. 17.
- Vaucouleurs, G. de, and Page, J. 1962, *Ap. J.*, **136**, 107.
- Vaucouleurs, G. de, and Malik, G. 1969, *M.N.R.A.S.*, **142**, 387.
- Watson, G. N. 1944, *A Treatise on the Theory of Bessel Functions* (2d ed.; Cambridge: Cambridge University Press).